The Journal of Chemical Physics

Coarse-grain molecular dynamics simulations of nanoparticle-polymer melt: Dispersion vs. agglomeration

Cite as: J. Chem. Phys. **138**, 144901 (2013); https://doi.org/10.1063/1.4799265
Submitted: 24 January 2013 . Accepted: 19 March 2013 . Published Online: 09 April 2013

Tarak K. Patra, and Jayant K. Singh

View Online Export Citation CrossMark

ARTICLES YOU MAY BE INTERESTED IN

Dynamics of entangled linear polymer melts: A molecular-dynamics simulation
The Journal of Chemical Physics **92**, 5057 (1990); https://doi.org/10.1063/1.458541

Perspective: Outstanding theoretical questions in polymer-nanoparticle hybrids
The Journal of Chemical Physics **147**, 020901 (2017); https://doi.org/10.1063/1.4990501

Effect of shear on nanoparticle dispersion in polymer melts: A coarse-grained molecular dynamics study
The Journal of Chemical Physics **132**, 024901 (2010); https://doi.org/10.1063/1.3277671

Challenge us.
What are your needs for periodic signal detection?
Watch

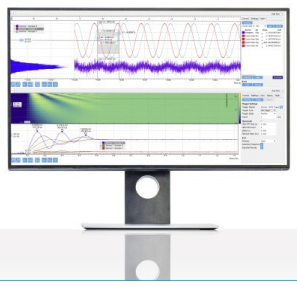

Zurich Instruments

© 2013 American Institute of Physics.

AIP Publishing

Coarse-grain molecular dynamics simulations of nanoparticle-polymer melt: Dispersion vs. agglomeration

Tarak K. Patra and Jayant K. Singh[a)]
Department of Chemical Engineering, Indian Institute of Technology Kanpur, Kanpur 208016, India

(Received 24 January 2013; accepted 19 March 2013; published online 9 April 2013)

In this work, we study the influence of polymer chain length (m), based on Lennard-Jones potential, and nanoparticle (NP)-polymer interaction strength (ε_{np}) on aggregation and dispersion of soft repulsive spherically structured NPs in polymer melt using coarse-grain molecular dynamics simulations. A phase diagram is proposed where transitions between different structures in the NP-polymer system are shown to depend on m and ε_{np}. At a very weak interaction strength $\varepsilon_{np} = 0.1$, a transition from dispersed state to collapsed state of NPs is found with increasing m, due to the polymer's excluded volume effect. NPs are well dispersed at intermediate interaction strengths ($0.5 \leq \varepsilon_{np} \leq 2.0$), independent of m. A transition from dispersion to agglomeration of NPs, at a moderately high NP-polymer interaction strength $\varepsilon_{np} = 5.0$, for $m = 1$–30, is identified by a significant decrease in the second virial coefficient, excess entropy, and potential energy, and a sharp increase in the Kirkwood-Buff integral. We also find that NPs undergo the following transitions with increasing m at $\varepsilon_{np} \geq 5.0$: string-like → branch-like → sphere-like → dispersed state. © *2013 American Institute of Physics*. [http://dx.doi.org/10.1063/1.4799265]

I. INTRODUCTION

Nanoparticles (NPs) are the potential candidates for altering the thermophysical properties of polymer solution.[1] For instance, spherical fullerene particles dispersed in amorphous polyethylene matrix enhance the elastic properties;[2] addition of a minute amount of silica particles is found to enhance the viscosity of polypropylene melt dramatically;[3] and alumina particles in water-ethylene glycol solution agglomerate into an elongated and dendrite-like structure which is found to be more efficient in enhancing the thermal conductivity than the spherical agglomerated phase.[4] Therefore, the thermophysical properties of NP-polymer solution largely depend on how NPs are arranged inside the fluid medium.[5] Thus, understanding the mechanism which governs the distribution of NPs in a polymeric solution is immensely important for the development of efficient technologies. Furthermore, the structured assemblies of NPs are potential candidates for multifunctional material and devices such as optoelectronic devices.[6] The assembling of NPs in polymer matrix depends on NP-polymer interaction,[7] temperature,[8] NP-polymer size ratio,[9] degree of polymerization,[10] NPs' volume fraction,[11] and pH of the medium.[12] All the parameters yield a preferential dominance or delicate balance between entropy and energy, which governs the assembly process and dispersion of NPs in the polymer matrix.

Computer simulations play an important role to explore the parameter space in polymer nanocomposite systems. Numerous molecular simulation studies have been done using coarse-grain models, derived from fully atomistic simulations.[13–17] These model systems have been quite successful in explaining many experimental observations.[18–26] In addition, various theoretic approaches such as mode coupling theory,[27,28] density functional theory,[29] self-consistent field theory,[30,31] and PRISM theory[32–34] have also been employed to study the polymer nanocomposites. The dispersion and agglomeration of NPs in the polymer matrix is shown to depend on the NP-polymer interaction strength.[24,33] NP-NP localization includes (i) direct contact aggregation, (ii) steric stabilization, (iii) local-bridging attraction, and (iv) long range "tele-bridging" attraction.[33] Direct contact aggregation takes place due to the fact that polymer entropy is higher away from the NP surface. The chain molecules tend to increase the excluded volume to maximize its entropy. It yields an entropic depletion attraction between NPs, which leads to the contact aggregation of NPs at a very weak NP-polymer interaction strength. As the interaction strength increases, steric stabilization takes place. Further increase in NP-polymer interaction strength leads to bridging of NPs via polymer layers.[33–35]

Most computer simulations have focused on the regimes of contact aggregation and dispersion of nanoparticles. Less attention has been given to the long range bridging of NPs which could form NP-polymer network. The aggregation of nanoparticles, sometimes, is of non-equilibrium nature, i.e., percolating gel-like structures,[14,15] which is sparsely studied. Furthermore, the effects of the degree of polymerization on the dispersion and aggregation of NPs are poorly understood, such as the mechanism of string-like, sphere-like, and branched-like aggregation of NPs, which depends on the polymer size and pH of the medium as reported in some of the recent experiments.[12,36–39] Even though the non-equilibrium studies are very few in the literature, the present work is an equilibrium study. Main objective of this work is to understand the NP-polymer network in detail employing molecular dynamics (MD) simulations with a structural representation of the NP using coarse-grain model. In addition, this work

a)Author to whom correspondence should be addressed. Electronic mail: jayantks@iitk.ac.in

 © 2013 American Institute of Physics

aims to illustrate the influence of the size of polymer on aggregation and dispersion of NPs in polymer melt systematically, by considering a wide range of polymer chain length and NP-polymer interaction strength, using MD simulations. In a recent work, Liu *et al*. has argued that the clustering of NPs at a strong NP-polymer interaction is governed by the entropic forces.[24] The entropic forces, by its nature, bring disorder in any system. Therefore, it is arguable to claim that the entropy leads to agglomeration of NPs in a polymer matrix, particularly when the polymer and NP are strongly interacting. We revisit the dispersion-aggregation mechanism with quantitative measurement of the entropy, potential of mean force, second virial coefficient (B_2), and the Kirkwood−Buff integrals (KBI) for the NPs distribution in polymer melts to reveal the correct mechanism of dispersion and agglomeration.

The rest of the paper is organized as follows. In Sec. II, we describe the model and simulation method in detail. Results and discussion are presented in Sec. III. Finally, the conclusions are drawn in Sec. IV.

II. MODEL AND METHOD

In this work, the polymers are modeled as linear chains. Each chain consists of coarse-grained beads; adjacent beads are connected through the FENE potential:[40]

$$V_{\mathrm{FENE}} = -0.5kR_0^2 \ln\left[1 - \left(\frac{r}{R_0}\right)^2\right], \tag{1}$$

where $R_0 = 1.5\sigma$ is a finite extensibility and $k = 30\varepsilon/\sigma^2$ is a spring constant. $V_{\mathrm{FENE}} = \infty$ when $r \geq R_0$. Here, σ is the monomer diameter and ε is the energy parameter. The choice of parameters prevents the crossing of chain. The dispersive interaction between any pair of beads is represented by the Lennard-Jones (LJ) potential:

$$V(r) = 4\varepsilon\left[\left(\frac{\sigma}{r}\right)^{12} - \left(\frac{\sigma}{r}\right)^{6}\right]. \tag{2}$$

The LJ potential is truncated and shifted at a cut off distance, $r_c = 2.2^{1/6}\sigma$. The NPs are modeled as rigid bodies. Each NP is made of 90 beads of size σ placed on the surface of a sphere of diameter 4σ. Thus, the size of a NP (D) is 5σ. All the beads are of equal mass which is same as that of a monomer unit of a polymer chain. The model is considered with the same spirit as proposed by Zhang and Glotzer.[41] This is a lower level of coarse-grain model which captures the roughness of NP surface to some extent, in comparison to single smooth sphere or bead depiction of NP. Any pair of beads from two different NPs interacts through Weeks-Chandler-Andersen (WCA) potential, Eq. (2), with $r_c = 2^{1/6}\sigma$. The beads of the same NP do not interact. The interaction between bead of NP and monomer unit of chain is attractive in nature and represented by Eq. (2) with $r_c = 2.5\sigma$.

The MD simulations are performed in a *NVT* ensemble. The monomer density is kept constant at $0.7\sigma^{-3}$. Several chain lengths, m, are considered, keeping the total number of monomer of solvent unchanged, which is fixed at 24000. Therefore, 800 chains are taken for the chain length $m = 30$, 2400 chains for $m = 10$, and 4800 chains for $m = 5$, etc. Total number of NPs in the system is 18 and the corresponding volume fraction is 0.034, as used by Liu *et al*.[24] The Nose-Hoover thermostat is applied to maintain the system temperature. It is known that phase transitions in NP-polymer system depend on the polymer size. For example, the vapor-liquid transition is observed when the radius of gyration of polymer is significantly larger than the size of the spherically colloid suspension. Fluid-solid transition, on the other hand, occurs for shorter chains.[42] Our main objective, in this work, is to study the structural properties of NP-polymer system in a liquid state for a wide range of chain length. All the simulations are performed in the liquid phase at $T = 2\varepsilon/k_B$, where k_B is the Boltzmann constant. The choice of temperature and density is such that all the chain lengths, considered in this study, are in liquid phase. The phase diagrams of different LJ chains can be found in Ref. 43. The velocity-verlet algorithm is used to integrate the equation of motions with time step $\Delta t = 0.001\tau$, where the unit of time $\tau = \sqrt{\varepsilon/m\sigma^2}$, m is the mass of a monomer unit. At each time step, the frozen subunits of a NP move together as a rigid body.[44] The initial configurations are melted at a very high temperature, $T = 5\varepsilon/k_B$, followed by a slow temperature tunneling to the desired temperature. In the tunneling process, the temperature is gradually reduced by 0.1 unit after 10^6 MD time steps until it reaches to $T = 2\varepsilon/k_B$. The systems are then equilibrated at the desired temperature for 2×10^7 steps followed by 10^7 production steps. The equilibrium time is long enough for the polymer to move at least twice the radius of gyration of the polymer, R_g, which is the equilibration criteria used in several works.[20,24] All the simulations are performed using the large-scale atomic/molecular massively parallel simulator (LAMMPS).[45] MD snapshots are generated using VMD molecular graphics package.[46]

III. RESULTS AND DISCUSSION

To explore the various possibilities of dispersion and aggregation of NPs, we consider a wide range of NP-polymer interaction strength, ε_{np}. Here, ε_{np} varies from 0.1 to 12.0 representing very weak to very strong attraction, respectively. We have represented the degree of polymerization by considering chain molecules of varying lengths, which takes into account all the three possible cases – (i) NP's radius is smaller than the radius of gyration of polymer, (ii) NP's radius and radius of gyration of polymer are of the same order, and (iii) NP's radius is larger than the radius of gyration of polymer.

First, we present the results for the polymer chain length $m = 30$. In a pure melt state without the NPs, the average radius of gyration of the system is $R_g = 2.73 \pm 0.58\sigma$ which is of the order of NP's radius. Figure 1 presents the radial distribution function (RDF) of NP-NP ($g_{nn}(r)$) in a polymer melt for $\varepsilon_{np} = 0.1$, 0.5, 1.0, and 5.0. The configuration snapshots for few ε_{np} values are given in Fig. 2. At $\varepsilon_{np} = 0.1$, the 1st peak of $g_{nn}(r)$ is at $r = 5\sigma$, which is the diameter of NP. This signifies that the NPs are in contact and they are in a collapsed state as clearly seen in Fig. 2. Therefore, there is a clear phase separation between the NPs and polymer melt. In case of slightly stronger interaction strength, $\varepsilon_{np} = 0.5$, we observe $g_{nn}(r)$ to exhibit a small peak at $r = 5\sigma$ before reaching its ideal value of unity from below. This indicates steric

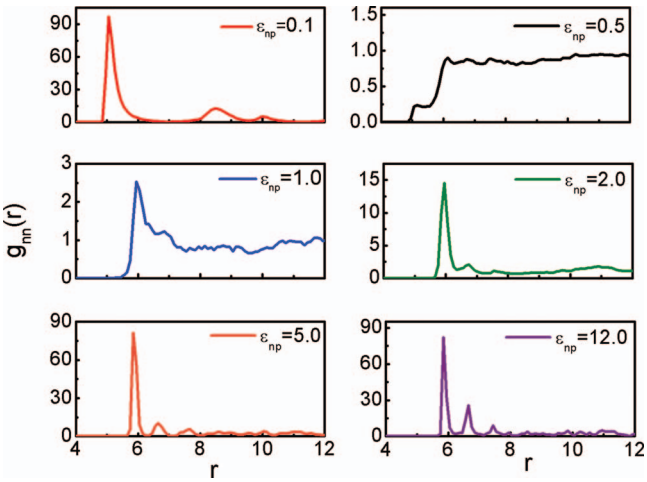

FIG. 1. The NP-NP RDFs, $g_{nn}(r)$, for $m = 30$, at different NP-polymer interaction strengths (ε_{np}).

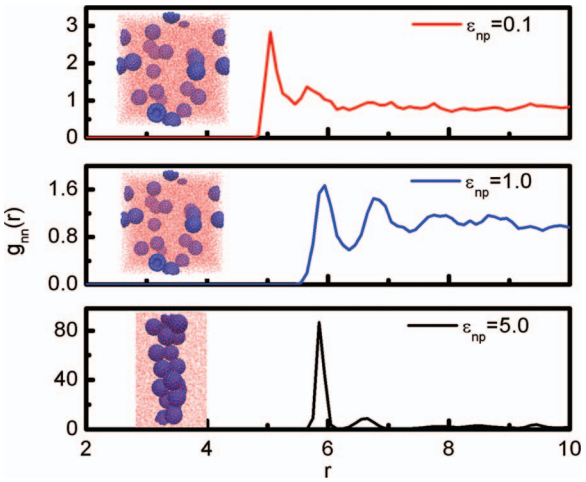

FIG. 3. The NP-NP RDFs, $g_{nn}(r)$, for $m = 1$, at different NP-polymer interaction strengths (ε_{np}). Representative snapshots corresponding to RDFs are shown in the inset of all the panels. The connectivity between adjacent beads of the chains is not shown for clarity.

stabilization of NPs as also predicted from the PRISM theory.[33] Increase in ε_{np} to 1.0 diminishes the direct contact between the NPs, leading to well-dispersed NPs throughout the medium. Further increase in ε_{np} increases the magnitude of the 1st peak of $g_{nn}(r)$ at $r = 6\sigma$. This is an indicative of large number of bridging of the NPs via the polymer chains. At considerably high interaction strength $\varepsilon_{np} = 5.0$, a structural transition occurs where all the NPs tend to agglomerate into a spherical-like aggregate as also evident from Fig. 2. This is also reflected in $g_{nn}(r)$ in the form of a drastic rise in the magnitude of the 1st peak at $r = 6\sigma$. At this state, all the NPs are connected via a single layer of polymers leading to NP-polymer network. The aggregation state achieved at $\varepsilon_{np} = 5.0$ is insensitive to further increases in ε_{np} as seen in

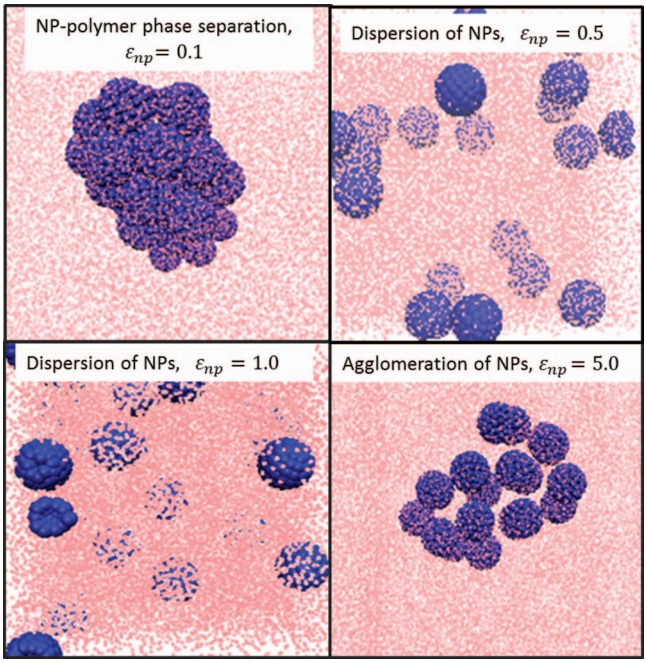

FIG. 2. The MD snapshots at different NP-polymer interaction strengths (ε_{np}) for $m = 30$. The connectivity between adjacent beads of chains is not shown for clarity.

$g_{nn}(r)$ for $\varepsilon_{np} = 12.0$, except for slight increase in the peaks of second and third coordination shells (see Fig. 1). This demonstrates the increment of two and three layers bridging of NPs. Clearly, the NPs and polymer form a structured network. Hence, with increasing ε_{np}, we observe the following transitions: collapsed state → dispersed state → aggregation state. This is also in agreement with the work of Liu *et al.*[24]

Now, we turn our attention to the case when the size of the NP is larger than that of the solvent. As a limiting size of the solvent, we consider monomer, i.e., $m = 1$. The $g_{nn}(r)$ for $m = 1$ is shown in Fig. 3 for various values of ε_{np}, along with its representative snapshots. The NPs and solvent do not phase separate completely at $\varepsilon_{np} = 0.1$, in contrast to the case of $m = 30$. Instead, we observe a mixed state with some of the NPs in smaller clusters forming contact segments and others in bridge segments corresponding to the first and second peaks (see Fig. 3) at $r = 5\sigma$ and 6σ, respectively. The contact segments and bridging segments are dispersed in the polymer matrix. Nonetheless, with increasing ε_{np} the behavior is similar to $m = 30$, except the transition to a string-like bridge network of NPs, which forms at $\varepsilon_{np} = 5.0$.

In the third case, $m = 50$, the radius of gyration of the pure melt ($\sim 3.62 \pm 0.75$) is much larger than the radius of NP. Figure 4 shows the $g_{nn}(r)$ along with the representative MD snapshot for different interaction strengths for $m = 50$. The NPs and polymer phase separate at weak NP-polymer interactions as evident for $\varepsilon_{np} = 0.1$. NPs are dispersed at intermediate interaction strengths, $0.5 \leq \varepsilon_{np} \leq 2.0$. The behavior at weak to moderate interaction strengths, for $m = 50$, is akin to that seen for $m = 30$. The effect of longer chain length, however, is noticed at very high interaction strengths, $\varepsilon_{np} \geq 5.0$, where NPs do not tend to agglomerate into a cluster. This is also reflected in the 1st peak height of the $g_{nn}(r)$, at the bottom panel of Fig. 4, which is considerably reduced compared to that seen for $m = 30$ (Fig. 1) and $m = 1$ (Fig. 3).

Now, we turn our attention to the roles of entropic and energetic contributions of different pairs, which lead to dispersion and agglomeration of NPs. Figure 5 presents the

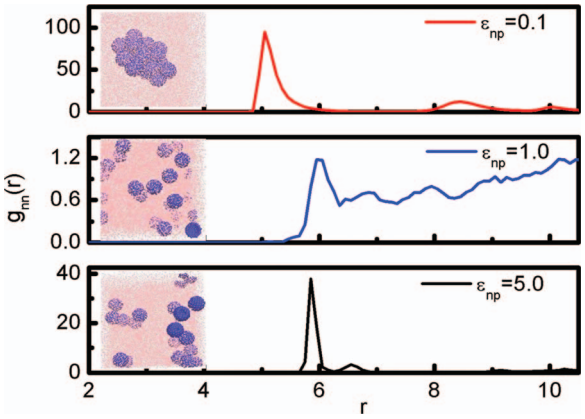

FIG. 4. The NP-NP RDFs, $g_{nn}(r)$, for $m = 50$, at different NP-polymer interaction strengths (ε_{np}). Representative snapshots corresponding to RDFs are shown in the inset of all the panels. The connectivity between adjacent beads of chains is not shown for clarity.

energy and entropy contribution of different pairs separately for $m = 30$. We calculate the excess entropy per particle within two-body approximation,[47] corresponding to pair distribution, which is written as $S_{ij} = -2\pi\rho\int\{g_{ij}(r)\ln g_{ij}(r) - (g_{ij}(r) - 1)\}r^2dr$ with i and j representing either NP or polymer. The two-body approximation is highly correlated with the total excess entropy as seen by Goel *et al.* for Lennard-Jones chains fluids.[48] Hence, the two-body entropy provides a reasonable estimate of the total excess entropy of the current system.[47,48] The NP-NP interaction energy (E_{nn}) is highest at $\varepsilon_{np} = 0.1$, where NPs are in contact (see Fig. 5). However, when the NPs move away from each other at $\varepsilon_{np} > 0.1$, E_{nn} decreases. We note that E_{nn} is zero for $\varepsilon_{np} \geq 0.5$, indicative of absence of direct NP-NP contact. S_{nn} is lowest at $\varepsilon_{np} = 0.1$, and with increasing ε_{np} it increases as NPs move away from each other. However, S_{nn} reaches its maximum at $\varepsilon_{np} = 1.0$ and it remains almost unchanged until $\varepsilon_{np} = 2.0$.

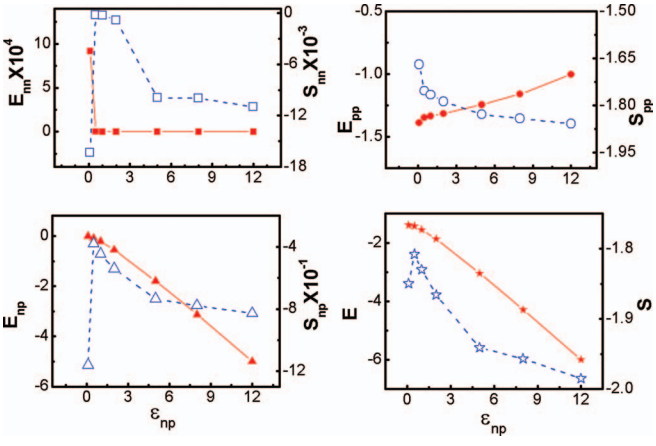

FIG. 5. The potential energies and entropic contributions of different pairs for $m = 30$ as a function of NP-polymer interaction strength (ε_{np}). Energy and entropy are shown on the left and right y-axes, respectively, in all the panels. E_{nn}, S_{nn}: NP-NP; E_{pp}, S_{pp}: polymer-polymer; E_{np}, S_{np}: NP-polymer. $E = E_{nn} + E_{pp} + E_{np}$. The symbols are the calculated values and lines serve as a guide to the eye. Closed symbols correspond to energy values and open symbols correspond to excess entropy values. The error bars are of the order of symbol sizes.

Subsequently, S_{nn} drops sharply with increase in ε_{np} from 2.0 to 5.0, as the system goes through a structural transition from a dispersed state to a state where NP-polymer network forms. We now look at the polymer-polymer contribution as shown in the top-right panel of Fig. 5. We note that the entropic contribution due to polymer-polymer interaction (S_{pp}) is highest at $\varepsilon_{np} = 0.1$, which is indicated by a small peak (maximum value in this case) in S_{pp} vs. ε_{np} plot. At this weak interaction strength, polymer does not mix with the NPs, as also seen in the snapshot (see Fig. 2) and it tends to maximize its configuration entropy. The NPs collapse at this weak interaction strength, as a result of polymer mediated entropic depletion interaction. As ε_{np} increases, S_{pp} slightly decreases first and subsequently remains almost unchanged. Similarly, the polymer-polymer pair energy (E_{pp}) is lowest at $\varepsilon_{np} = 0.1$ and increases gradually with increasing ε_{np}. The NP-polymer pair energy (E_{np}) on the other hand decreases with increasing ε_{np} as shown in the bottom-left panel of Fig. 5. The entropy due to NP-polymer interaction (S_{np}), on the contrary, shows a maximum when the polymer and NPs are well mixed at $\varepsilon_{np} = 0.5$ and it decreases with further increase in ε_{np}. Overall, the total energy ($E = E_{nn} + E_{np} + E_{pp}$) decreases with increasing ε_{np}. The total excess entropy of NP-polymer system can be calculated, within two-body approximation as $S = -2\pi\rho\sum_{ij} x_i x_j \int\{g_{ij}(r)\ln g_{ij}(r) - (g_{ij}(r) - 1)\}r^2dr$, where x_i and x_j are the mole fractions of ith and jth components, respectively.[49] S is found to be low at $\varepsilon_{np} = 0.1$ when polymer–NPs phase separate. It increases to a maximum value when NP and polymer are well mixed at $\varepsilon_{np} = 0.5$. Subsequently, it decreases with increasing ε_{np}, leading to bridging of NPs. However, in this low NP volume fraction limit, the variation of S as a function of ε_{np} is not drastic, as seen in Fig. 5. The mean square deviation in S_{pp} calculated at different ε_{np} is 3%; however, it is 107% and 35% in S_{nn} and S_{np}, respectively. Further, S_{nn} and S_{np} behavior is alike with increasing ε_{np}. But, S changes by a maximum of only 4%, considering all the cases studied in this work. S_{nn} is found to be most sensitive with the change in NP-polymer interaction strength. Therefore, S_{nn} is the most significant and important quantity to understand the NP-polymer system, when the NPs volume fraction is very low. To this end, we study the potential energy per particle (E), along with the entropic contribution due to NP-NP distribution (S_{nn}), to analyze the physical properties of NP-polymer system.

The potential of mean force (PMF), 2nd virial coefficient, and KBI are also estimated, along with energy and entropy. The PMF of NP-NP distribution can be evaluated as $V_{PMF}(r) = -k_BT\ln(g_{nn}(r))$,[50] and the corresponding 2nd virial coefficient is $B_2 = -\frac{1}{2}\int_0^\infty [\exp(-\beta V_{PMF}(r)) - 1]4\pi r^2dr$. Here, B_2 is the effective perturbation from ideal NPs to NP-polymer system which has significant particle-particle interaction due to the interparticle forces and effective induced forces from the solvent, i.e., polymer matrix. The B_2 is essentially a measure of the tendency of NPs to disperse or aggregate within the system. A positive value of B_2 indicates repulsive force between the NPs, which prevents any phase separation in the system. On the other hand, a negative value of B_2 is indicative of attraction among the NPs, which may lead NPs and polymer to phase

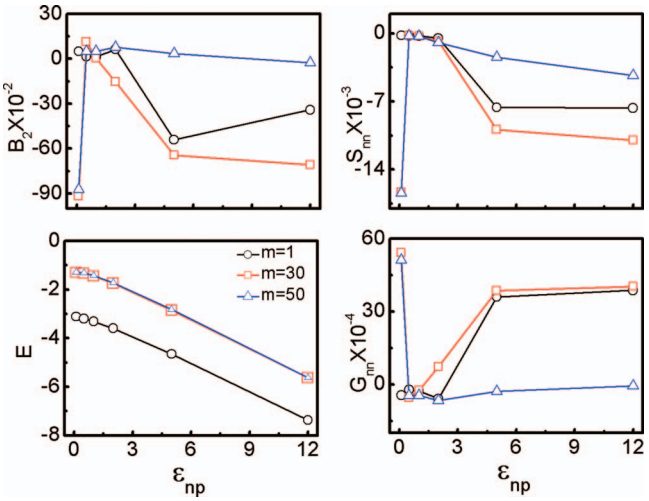

FIG. 6. The 2nd virial coefficient (B_2), excess entropy (S_{nn}), potential energy (E), and KBI (G_{nn}), as a function of ε_{np}, are shown for $m = 1$, 30, and 50. The symbols are the calculated values and lines serve as a guide to the eye. The error bars are of the order of symbol sizes.

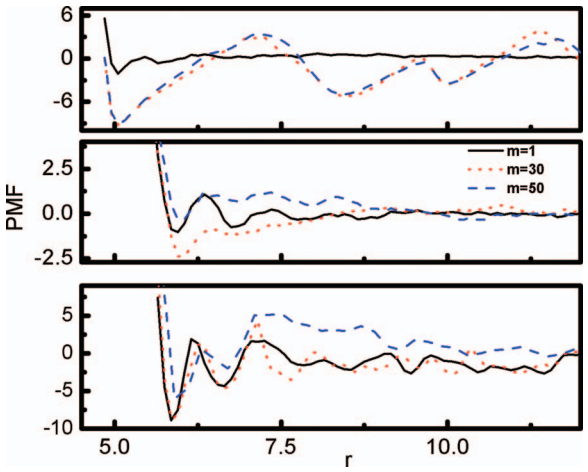

FIG. 7. Potential of mean force (PMF) as a function of inter-particle distance for $m = 1$, 30, and 50. Top panel corresponds to $\varepsilon_{np} = 0.1$, middle panel corresponds to $\varepsilon_{np} = 1.0$, and the bottom panel corresponds to $\varepsilon_{np} = 5.0$.

separate. The KBI for the NP-NP distribution is calculated as $G_{nn} = 4\pi \int_0^\infty [g_{nn}(r) - 1]r^2 dr$.[51] As evident from the similarity of the above expression with that of B_2, the KBI also represents the affinity among NPs. KBI provides the information about the strength of the NP-NP interaction similar to B_2.

Figure 6 presents B_2, S_{nn}, E, and G_{nn} for different ε_{np} values for all three cases. The B_2 attains a large negative value at $\varepsilon_{np} = 0.1$, for $m = 30$ and 50. This clearly indicates that NPs are attractive, and remain in a separate phase, at $\varepsilon_{np} = 0.1$. In contrast, B_2 for $m = 1$ at $\varepsilon_{np} = 0.1$ is close to zero, where NPs remain dispersed in the medium. As ε_{np} slightly increases to 0.5, B_2 becomes positive and NPs are well dispersed in the medium, for $m = 30$ and 50. The NP-polymer dispersed state at an intermediate range $\varepsilon_{np} = 0.5-1.0$ is independent of the polymer chain length. B_2 becomes negative at higher $\varepsilon_{np} > 1.0$, which represents the tendency of NPs to draw closer. The behavior changes again at a high NP-polymer interaction strength, $\varepsilon_{np} \geq 5.0$, where B_2 decreases sharply to a very large negative value, and NP-polymer network forms in case of $m = 1$ and 30. However, for $m = 50$, where polymer size is bigger than NP's size, B_2 is greater than that for the case of $m = 1$ and 30. In this case, NPs do not come close to form any structured cluster. The behavior seen in the second virial coefficient is also reflected in the S_{nn} values as shown in the top-right panel of Fig. 6. The lowest S_{nn}, for $m = 30$ and 50, is at $\varepsilon_{np} = 0.1$, as NPs and polymer phase separate. In case of $m = 1$, NPs and polymer are well mixed at this point and entropy is high. Slight increase in ε_{np} to 0.5, for $m = 30$ and 50, leads to drastic jump in S_{nn} as NPs are now in the dispersed state. In the intermediate range $\varepsilon_{np} = 0.5-1.0$, i.e., in the dispersed state, S_{nn} is not sensitive to the polymer chain length. However, S_{nn} drops significantly with a change in ε_{np} from 2.0 to 5, akin to that seen in B_2. At this interaction strength, system undergoes a structural transition also reflected in the MD snapshots of Figs. 2 and 3. Accordingly, energy (see the bottom-left panel of Fig. 6) shows a sharp decrease, when ε_{np} changes from 2.0 to 5.0. Therefore, the transition is energy driven. The structural transition with NP-polymer interaction strength and polymer chain length is also reflected in the Kirkwood-Buff integral values, G_{nn}. For example, G_{nn}, at $\varepsilon_{np} = 0.1$, is highest for $m = 30$ and 50 corresponding to the complete phase separation between the NPs and polymer melt. On the other hand G_{nn}, at $\varepsilon_{np} = 0.1$, is lowest for $m = 1$ representing the dispersion of NPs. On the whole, G_{nn} behavior is a mirror image of B_2. Therefore, we infer that the decrease in B_2, S_{nn}, and E, and the increase in G_{nn} at large NP-polymer interaction strengths represent the agglomeration tendency of NPs. The agglomeration tendency leads to a structural transition in the system to form NP-polymer network.

Now, we will investigate the nature of NP-polymer networks which form at strong NP-polymer interaction strength. Our calculations are equilibrium in nature; however, it has implication of non-equilibrium phenomena such as gelation. The polymer mediated gelation or percolation network formation can be identified with the emergence of a minimum in PMF deeper than -3 to -4 k_BT,[33,52,53] k_B and T are Boltzmann constant and temperature, respectively. Figure 7 represents PMF between NPs in three different regions – weak NP-polymer interaction strength (top panel), intermediate NP-polymer interaction strength (middle panel), and very strong NP-polymer interaction strength (bottom panel). In all the cases, we have seen attractive potential barriers. In the first panel, at $\varepsilon_{np} = 0.1$, the minimum of PMF is ~ -10 k_BT for $m = 30$ and 50. The minimum is observed at $r = 5.0\sigma$, which indicates the contact aggregation of NPs. Therefore, there is no polymer layer in between NPs, i.e., NP-polymer network does not form. Hence, the agglomeration is equilibrium clustering. This observation is in line with the PRISM theory prediction of Hooper and Schweizer.[34] In the middle panel, at $\varepsilon_{np} = 1.0$, the depth of the attractive potential well is ~ -2.5 k_BT and the minimum takes place at $r = 6.0\sigma$. It is the signature of layer in between NPs, which are again equilibrium structures. In the bottom panel, we have shown the PMF for a very strong NP-polymer interaction strength, $\varepsilon_{np} = 5.0$. The minimum is deeper than -4 k_BT, irrespective of the chain length, which is the signature of percolating network. NP-polymer network

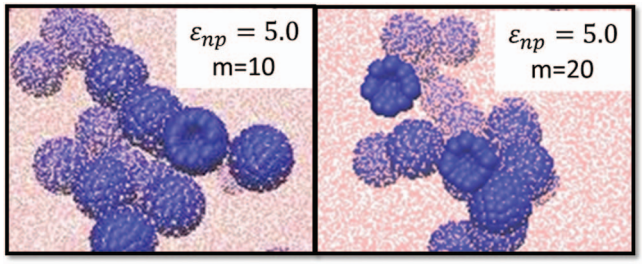

FIG. 8. Two branch structures of NPs at different state points as mentioned in the figure. The connectivity between adjacent beads of chains is not shown for clarity.

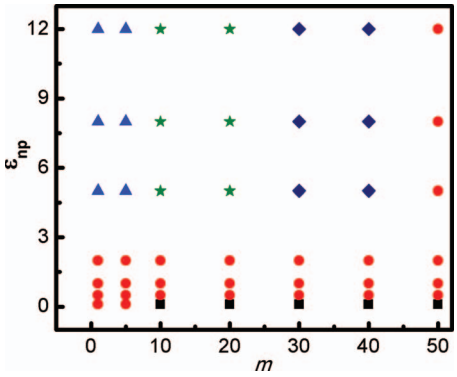

FIG. 9. Predicted ε_{np} vs. m phase diagram of NP-polymer system. Symbols represent the phases as follows: (■) NPs and polymer melt phase separate, (●) NPs disperse in the polymer melt, (▲) string-like assembly of NPs, (★) branch structure of NPs, (⧫) spherical shape assemblies of NPs.

forms due to tight bridging of NPs via polymer. Therefore, we expect that at very strong NP-polymer interaction strengths the agglomerations are non-equilibrium structures.

To this end, our conclusion pertaining to the transition at $\varepsilon_{np} = 5.0$ or higher is in disagreement with the speculation of Liu *et al.*[24] who concluded that the transition from NPs dispersion to NPs agglomeration is entropy dominated. The authors did not report the entropy values, and the speculation was based on monitoring the system's enthalpy, when NP-polymer interaction strength is changed from intermediate ($\varepsilon_{np} = 2.0$) to a very high value ($\varepsilon_{np} = 5.0$). The authors noticed insignificant change in enthalpy for the period of time, 500τ, in an isobaric isothermal ensemble. We attribute this disagreement to the differences in simulation run length, coarse-grain model of the NP, and temperature of the system. Considering the above, the similarity between aggregates observed in this work and that of Liu *et al.*[24] is puzzling, and possibly, is a coincidence. In this work, we clearly notice a decrease in entropy and energy when ε_{np} changes from 2.0 to 5.0. We conclude that the transition from two separate phases to a well-mixed state of the NPs and the polymer chains is dominated by entropy of the system. However, at higher interaction strength, the transition from well-mixed state to agglomeration state of NPs is driven by the energy of the NP-polymer system.

We further explore the parameter space to understand all the possible structures. There exist few branch structures in between the string-like and sphere-like assemblies, at an intermediate chain length ($5 < m < 30$), and strong NP-polymer interaction ($\varepsilon_{np} \geq 5.0$). Figure 8 presents two examples of observed branch structures. Branch structures are also observed in experimental studies such as for silica-latex system[54,55] and PEO-modified C60 Fullerene.[56] We summarize all possible structures of the NP-polymer system in a phase diagram, shown in Fig. 9. The transition from collapsed NPs to dispersed NPs in the polymer melt at a lower value of ε_{np} is akin to that predicted from the PRISM theory.[33] When ε_{np} increases from an intermediate value to a high value, the system moves to a new state where NPs and polymer form percolating network. However, the network changes its shape with the chain length. For, $m = 1$, it is string-like. As m increases, the network is found in a branch structure. Further increase in m to 30, where radius of gyration of chain and NP's radius are of the same order, the network is sphere-like. As polymer size becomes greater than NP's size, the aggregation tendency of NPs is very poor as seen for the case of $m = 50$. This observation is in agreement with a recent experiment where Au NPs are shown to aggregate in a short polystyrene medium, and an energy barrier induced by the long chain leads to poor aggregation.[10]

IV. CONCLUSIONS

In this work, we perform molecular dynamics simulations using a coarse-grain model of nanoparticle to understand the structures and transitions of NP-polymer system. Our results explain experimentally observed structures and their transitions using a quantitative measurement of entropy, internal energy, second virial coefficient, and Kirwood-Buff integral. This work illustrates the agglomeration and dispersion mechanisms of NPs in polymer melt for a wide range of interaction strength and degree of polymerization. The dispersion of NPs in the polymer melt is governed by the entropy of the system. On the other hand, internal energy dominates to agglomerate NPs, leading to polymer directed assemblies of NPs. It is found that, at a very weak NP-polymer interaction strength, phase separation may occur if the polymer size is above a critical value. At an intermediate interaction, NPs are found to be well dispersed in polymer melt irrespective of the radius of gyration of polymer melt. At a very strong interaction, there is a transition from a string-like agglomeration to a spherical agglomeration via a series of branch objects, as the degree of polymerization increases. However, when the radius of gyration of the polymer is larger than the radius of NP, NPs do not agglomerate. The two possible structures for very long chain polymer are – phase separation at very weak interaction and dispersion of NPs for a wide range of interaction strength.

We present a phase diagram of possible structures, depending on the degree of polymerization and polymer-NP interaction strength. The phase diagram which is proposed based on our coarse-grain molecular dynamics simulations will help to develop a general strategy to control and direct the assembly of NPs in polymer matrix.

ACKNOWLEDGMENTS

This work is supported by the Department of Science and Technology (DST), Government of India. The computational facilities are provided from the Centre for Development of Advance Computing (CDAC), Pune, India. T.K.P. thanks the Council of Scientific and Industrial Research (CSIR), Government of India for supporting this work in terms of a senior research fellowship. J.K.S. wishes to thank Evangelos Voyiatzis for fruitful discussions.

[1] S. M. S. Murshed, K. C. Leong, and C. Yang, Appl. Therm. Eng. **28**, 2109 (2008).
[2] A. Adnan, C. T. Sun, and H. Mahfuz, Compos. Sci. Technol. **67**, 348 (2007).
[3] S. Jain *et al*., Soft Matter **4**, 1848 (2008).
[4] E. V. Timofeeva *et al*., Phys. Rev. E **76**, 061203 (2007).
[5] R. Prasher, Nano Lett. **6**, 1529 (2006).
[6] E. Ozbay, Science **311**, 189 (2006).
[7] V. V. Ginzburg and A. C. Balazs, Adv. Mater. **12**, 1805 (2000).
[8] A. K. Boal *et al*., Nature (London) **404**, 746 (2000).
[9] M. E. Mackay *et al*., Science **311**, 1740 (2006).
[10] N. Biswas and A. Datta, Chem. Phys. Lett. **531**, 177 (2012).
[11] M. A. Horsch, Z. Zhang, and S. C. Glotzer, Phys. Rev. Lett. **95**, 056105 (2005).
[12] S. Zhou *et al*., Langmuir **28**, 13181 (2012).
[13] B. Hong, A. Chremos, and A. Z. Panagiotopoulos, J. Chem. Phys. **136**, 204904 (2012).
[14] A. Kutvonen *et al*., J. Chem. Phys. **137**, 214901 (2012).
[15] A. Kyrychenko *et al*., Comput. Theor. Chem. **977**, 34 (2011).
[16] A. Striolo *et al*., J. Phys. Chem. B **111**, 12248 (2007).
[17] R. Chang and J. Lee, Bull. Korean Chem. Soc. **31**, 3195 (2010).
[18] F. W. Starr, J. F. Douglas, and S. C. Glotzer, J. Chem. Phys. **119**, 1777 (2003).
[19] A. J. Rahedi, J. F. Douglas, and F. W. Starr, J. Chem. Phys. **128**, 024902 (2008).
[20] T. Desai, P. Keblinski, and S. K. Kumar, J. Chem. Phys. **122**, 134910 (2005).
[21] F. L. Verso *et al*., J. Chem. Phys. **135**, 214902 (2011).
[22] L.-T. Yan *et al*., Soft Matter **7**, 595 (2011).
[23] C. R. Iacovella and S. C. Glotzer, Nano Lett. **9**, 1206 (2009).
[24] J. Liu *et al*., Langmuir **27**, 7926 (2011).
[25] P. Akcora *et al*., Nature Mater. **8**, 354 (2009).
[26] M. Goswamia and B. G. Sumpter, J. Chem. Phys. **130**, 134910 (2009).
[27] S. A. Egorov, J. Chem. Phys. **134**, 084903 (2011).
[28] S. M. Bhattacharyya, Chem. Phys. Lett. **386**, 83 (2004).
[29] N. Patel and S. A. Egorov, J. Chem. Phys. **121**, 4987 (2004).
[30] S. A. Egorov and K. Binder, J. Chem. Phys. **137**, 094901 (2012).
[31] D. M. Trombly and V. Ganesan, J. Chem. Phys. **133**, 154904 (2010).
[32] J. B. Hooper *et al*., J. Chem. Phys. **121**, 6986 (2004).
[33] J. B. Hooper and K. S. Schweizer, Macromolecules **38**, 8858 (2005).
[34] J. B. Hooper and K. S. Schweizer, Macromolecules **39**, 5133 (2006).
[35] J. B. Hooper and K. S. Schweizer, Macromolecules **40**, 6998 (2007).
[36] Y. Kang, K. J. Erickson, and T. A. Taton, J. Am. Chem. Soc. **127**, 13800 (2005).
[37] M. Fukao *et al*., J. Am. Chem. Soc. **131**, 16344 (2009).
[38] S. Srivastava and N. A. Kotov, Soft Matter **5**, 1146 (2009).
[39] Z. Tang and N. A. Kotov, Adv. Mater. **17**, 951 (2005).
[40] G. S. Grest and K. Kremer, Phys. Rev. A **33**, 3628 (1986).
[41] Z. Zhang and S. C. Glotzer, Nano Lett. **4**, 1407 (2004).
[42] E. J. Meijer and D. Frenkel, J. Chem. Phys. **100**, 6873 (1994).
[43] F. J. Blas *et al*., J. Chem. Phys. **129**, 144703 (2008).
[44] T. F. Miller *et al*., J. Chem. Phys. **116**, 8649 (2002).
[45] S. J. Plimpton, J. Comput. Phys. **117**, 1 (1995).
[46] W. Humphrey, A. Dalke, and K. Schulten, J. Mol. Graphics **14**, 33 (1996).
[47] A. Baranyai and D. J. Evans, Phys. Rev. A **40**, 3817 (1989).
[48] T. Goel *et al*., J. Chem. Phys. **129**, 164904 (2008).
[49] B. B. Laird and A. D. J. Haymet, J. Chem. Phys. **97**, 2153 (1992).
[50] J. S. Smith, D. Bedrov, and G. D. Smith, Compos. Sci. Tech. **63**, 1599 (2003).
[51] J. G. Kirkwood and F. P. Buff, J. Chem. Phys. **19**, 774 (1951).
[52] L. M. Hall and K. S. Schweizer, J. Chem. Phys. **128**, 234901 (2008).
[53] W. C. K. Poon, J. Phys.: Condens. Matter **14**, R859 (2002).
[54] J. Oberdisse, Soft Matter **2**, 29 (2006).
[55] J. Oberdisse, P. Hine, and W. Pyckhout-Hintzen, Soft Matter **3**, 476 (2007).
[56] J. B. Hooper, D. Bedrov, and G. D. Smith, Langmuir **24**, 4550 (2008).